Supplementary Information

Induced chirality in metal porphyrin–based biomimetic catalysts promotes ORR activity by enabling spin-polarization effects

Anujit Balo, Utkarsh Utkarsh, Mive Yasmin, Koyel Banerjee Ghosh*

Department of Chemistry, Indian Institute of Technology Hyderabad, Telangana 502284, India

Corresponding Author

Koyel Banerjee Ghosh

Email: koyel@chy.iith.ac.in

Experimental methodology

1. Materials

Benzaldehyde (SRL, 99%), propionic acid (SRL, 99.5%), pyrrole (SRL, 99%), cobalt (II) acetate tetrahydrate ($Co(OAc)_2.4H_2O$, SRL, 99%), iron chloride ($FeCl_3$, Sigma Aldrich, 97%), chloroform (SRL, 99.5%), N,N-dimethylformamide (DMF, SRL, 99.5%), methanol (Thermo Fisher scientific), hydrochloric acid (HCl, Finar, 35-38%), dichloromethane (DCM, SRL, 99.5%), (+)-10-camphor sulfonic acid (TCI, >98%), (-)-10-camphor sulfonic acid (TCI, >98%), (±)-10-camphor sulfonic acid (TCI, >98%), carbon black super P conductive 99 (Thermo Fisher scientific). All the chemicals are commercially available and used without further purification. For the washing processes and all the electrolytes preparation, milli-Q water is used.

2. Synthesis of metal free meso-tetraphenylporphyrin moiety (H_2TPP)

The synthesis procedure of the metal free porphyrin moiety was carried out based on the method described in earlier reports.[1] In a typical synthesis methodology, a mixture containing benzaldehyde (8 mL) and propionic acid (300 mL) was refluxed at 130 °C, thereafter, pyrrole (5.6 mL) was added to the mixture and further refluxed at 140 °C with continuous stirring for 1 hour. After cooling down to room temperature, a dark violet solid, meso-tetraphenylporphyrin (H_2TPP) was obtained by filtration and thoroughly washed with methanol.

3. Synthesis of cobalt (II) tetraphenylporphyrin (CoTPP)

The insertion of metal into the cavity of H_2TPP was achieved by adding cobalt(II) acetate tetrahydrate (622 mg) into the mixture containing H_2TPP (232 mg), chloroform (12 mL) and propionic acid (12 mL) and refluxed at 120 °C with stirring for 1.5 hours. After cooling down to ambient temperature, the brown color solid, cobalt (II) tetraphenylporphyrin (CoTPP) was obtained through filtration and methanol washing.

4. Synthesis of iron (III) tetraphenylporphyrinato chloride (FeTPPCl)

The synthesis of FeTPPCl was carried out by following the previously reported procedure with minor modifications.[2] Typically, H_2TPP and $FeCl_3$ were dissolved in N, N-dimethylformamide (45 mL) in 1:3 ratio and the mixture was refluxed at 150 °C for 5 hours. Then, the solution was further stirred under ice bath for another 2 hours. An immediate appearance of solid was

observed with the addition of cold water (45 mL). Finally, the blue-violet solid, FeTPPCl, was extracted by filtration and followed by the successive washing with 3 M HCl and milli-Q water.

5. Instrument used to characterize the metalloporphyrin moiety (CoTPP and FeTPPCl)

The formation of the metalloporphyrin moieties was initially confirmed from the ultraviolet-Visible (UV-Vis) spectra measured in JASCO V-730 spectrophotometer (scan range of 250 - 800 nm and 200 nm/min scan rate) using DCM as a solvent. The crystalline nature of the molecules was analysed by X-ray diffraction (XRD) technique using Malvern PANalytical Empyrean Powder XRD device. The internal structural analogy was examined by Fourier transform infrared (FTIR) and Raman spectroscopy techniques. Bruker Alpha-P Fourier Transform spectrophotometer and WITec alpha 300 Raman imaging microscope (excitation wavelength of 532 nm) were used for FTIR and Raman study, respectively. The X-ray photoelectron spectroscopy (XPS) was carried out in AXIS SUPRA system. The circular dichroism (CD) technique with JASCO spectrophotometer was used for the polarizability difference between chiral and racemic camphorsulfonic acid (CSA).

6. Determination of Kinetics assessments

The kinetic assessments were evaluated from the Koutecky–Levich (KL) plots using the KL equation (1)-(3)

$$\frac{1}{j} = \frac{1}{j_l} + \frac{1}{j_k} = \frac{1}{j_k} + \frac{1}{B\omega^{1/2}} \tag{1}$$

$$B = 0.62nFC_0D_0^{2/3}\nu^{-1/6} \tag{2}$$

$$j_k = \frac{(j \times j_l)}{(j_l - j)} \tag{3}$$

where, j, j_l, and j_k are measured current density (mA cm^{-2}), limiting current density (mA cm^{-2}) and kinetic current density (mA cm^{-2}), respectively. ω is the electrode angular rotation rate (rad s^{-1}). n is the electron transfer number, F is the Faraday constant (96,485 C mol^{-1}). The other terms, like C_0 is the bulk oxygen concentration (1.20×10^{-6} mol cm^{-3} in 0.1 M $HClO_4$ and 1.26

$\times 10^{-6}$ mol cm^{-3} in 0.1 M KOH), D_0 is the diffusion coefficient of oxygen molecules (1.90×10^{-5} cm^2 s^{-1} in 0.1 M $HClO_4$ and 1.98×10^{-5} cm^2 s^{-1} in 0.1 M KOH), and ν is the kinetic viscosity of the electrolytes (0.01 cm^2 s^{-1} in 0.1 M $HClO_4$ and 0.01 cm^2 s^{-1} in 0.1 M KOH).[3] The half-wave potential ($E_{1/2}$) value was estimated considering the potential of half of the average limiting current density at 0.60-0.20 V vs RHE for 0.1 M KOH and 0 V to -0.20 V vs RHE for 0.1 M $HClO_4$. The kinetic current density (mA cm^{-2}) was calculated using the equation (3) at $E_{1/2}$ region and the mass activity (A g^{-1}) was calculated by normalizing the kinetic current density with the loaded mass.

1. Structural characterization of the metalloporphyrin moiety

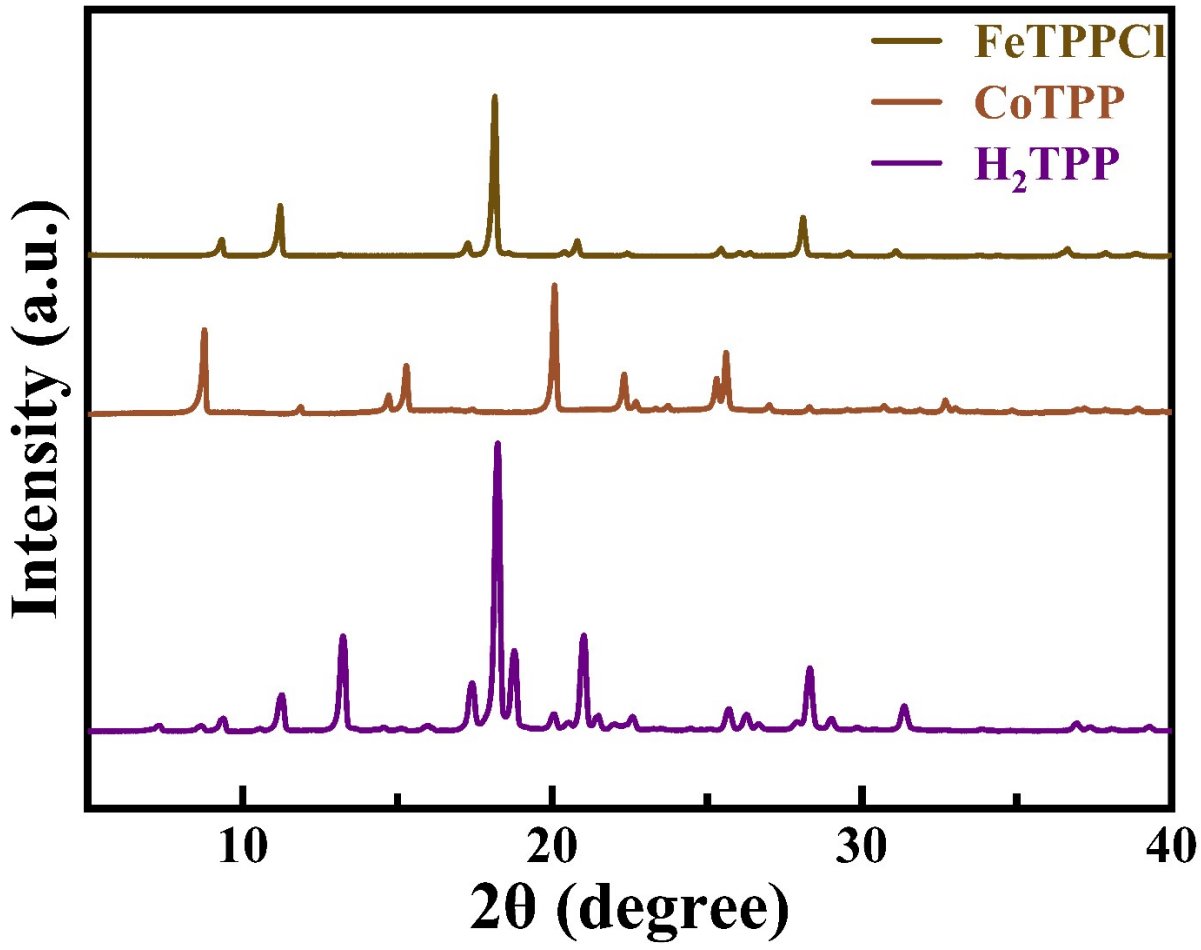

Figure S1. XRD spectra of H_2TPP, CoTPP, and FeTPPCl.

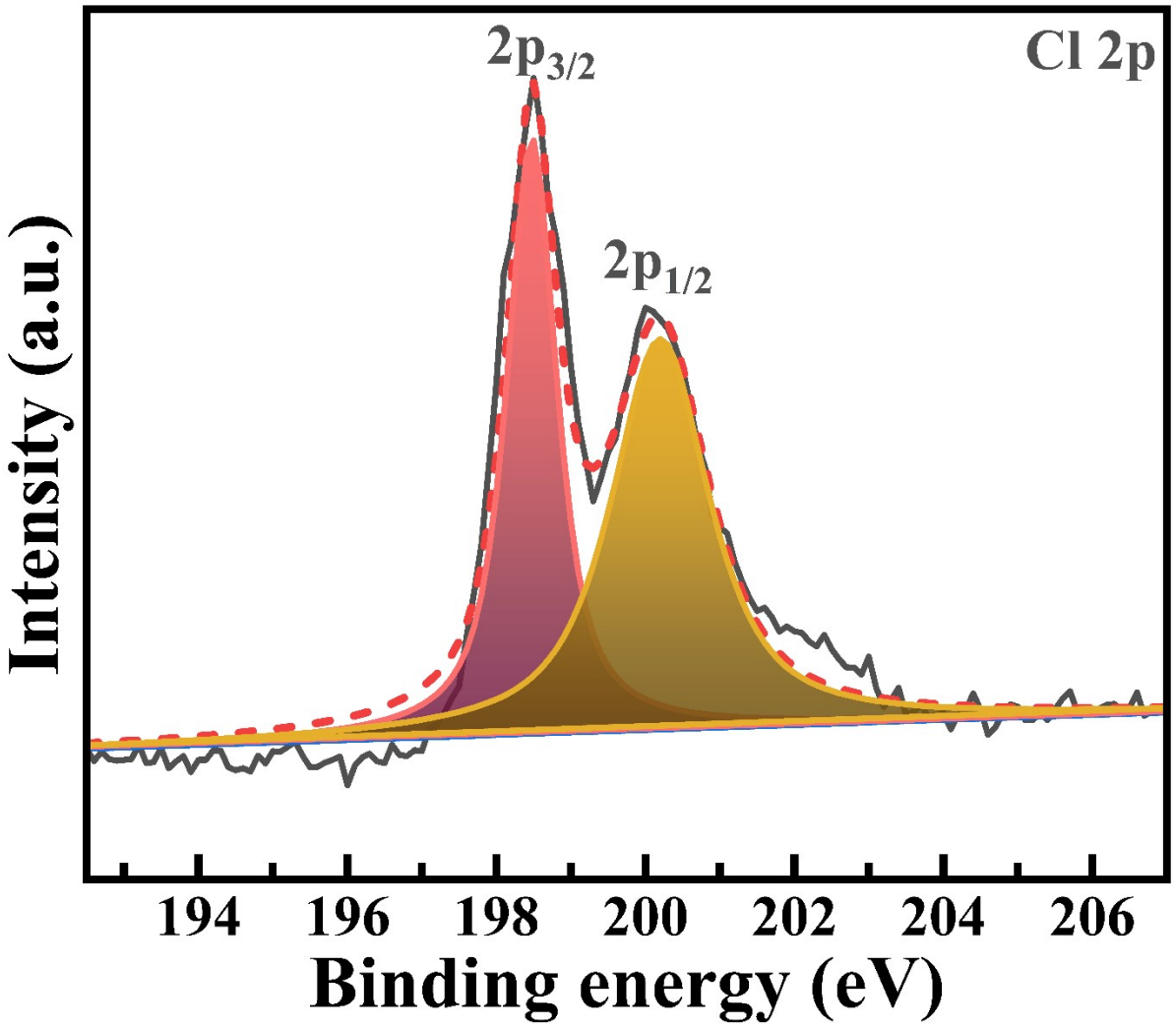

Figure S2. XPS high resolution Cl 2p spectrum of FeTPPCl.

2. Kinetics analysis in alkaline medium

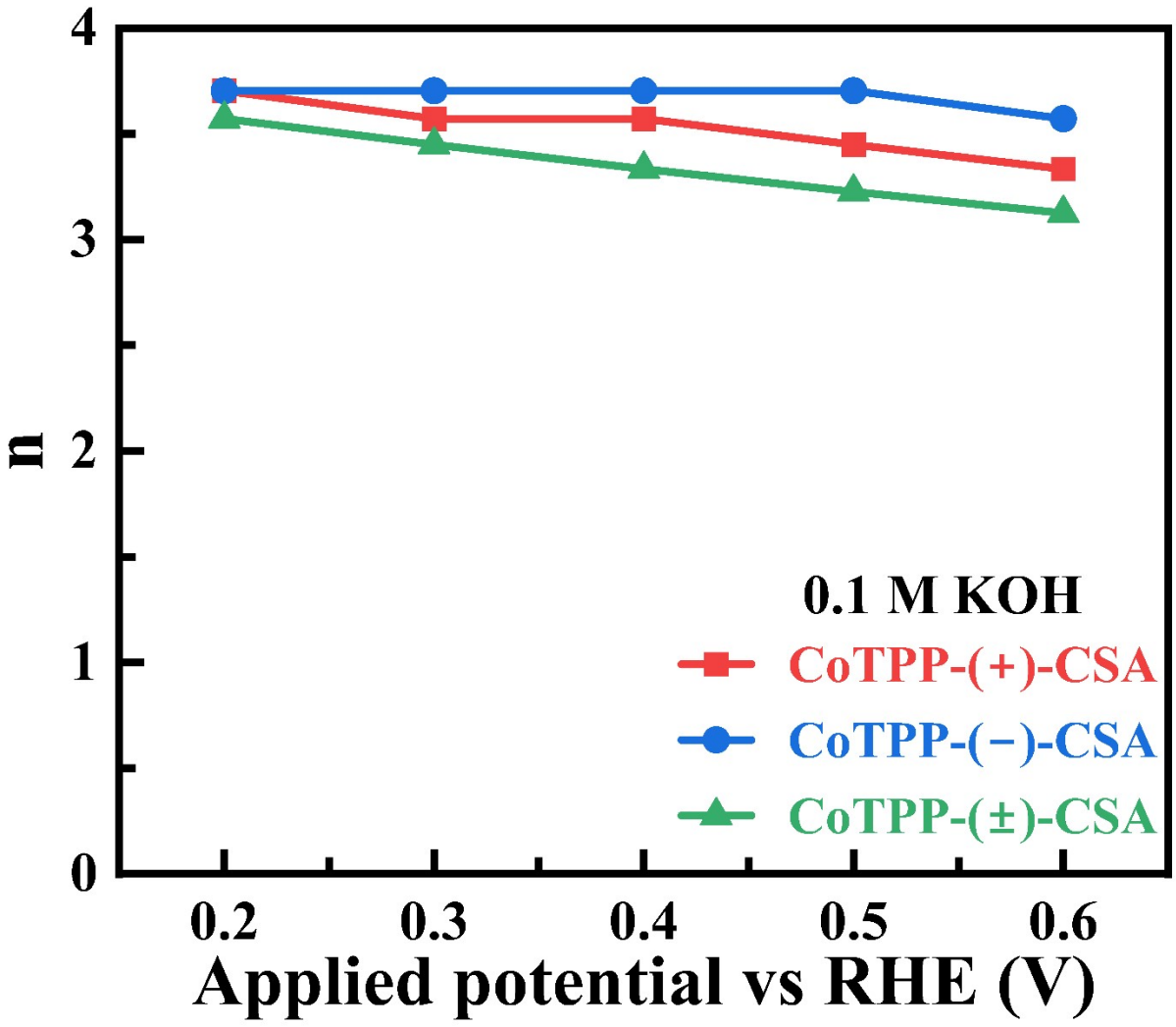

Figure S3. Electron transfer number for chiral ((+)/(-)) and racemic (±)-CSA assembled CoTPP under alkaline (0.1 M KOH) environment.

3. Electrochemical assessment of chiral and racemic-CSA assembled CoTPP in acidic medium

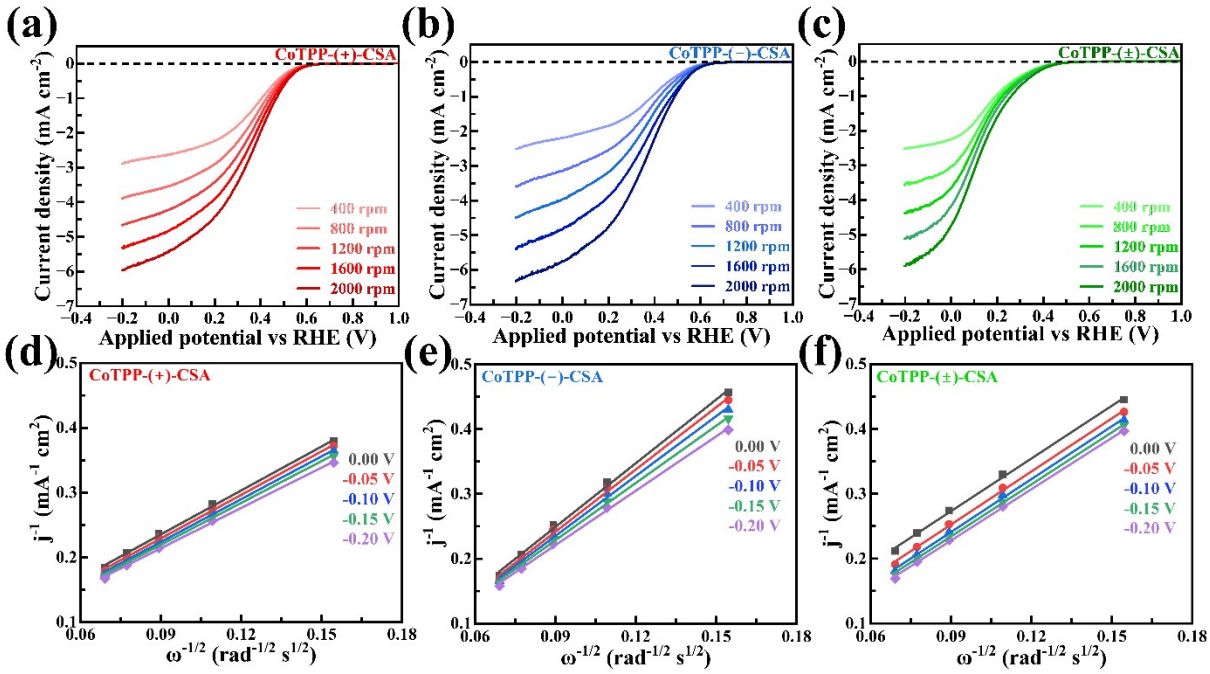

Figure S4. Cathodic polarization plots at different rpm and corresponding KL plots at different potentials in mass transport region for (a, d) CoTPP-(+)-CSA, (b, e) CoTPP-(-)-CSA, and (c, f) CoTPP-(±)-CSA under O_2-saturated 0.1 M $HClO_4$ environment.

4. Kinetics analysis in acidic medium

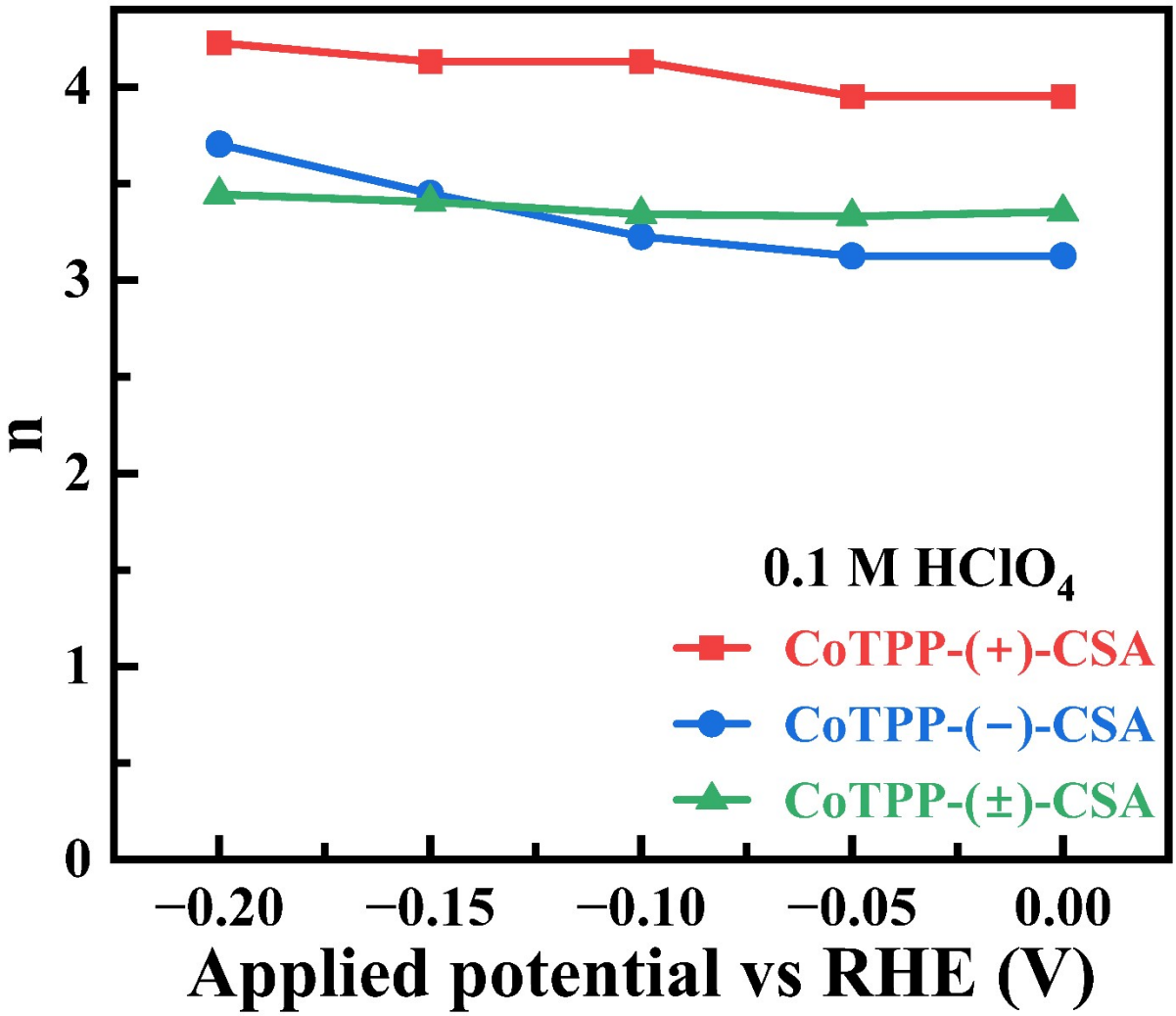

Figure S5. Electron transfer number for chiral ((+)/(-)) and racemic (±)-CSA assembled CoTPP under acidic (0.1 M $HClO_4$) environment.

5. Electrochemical assessment of chiral and racemic-CSA assembled FeTPPCl in acidic medium

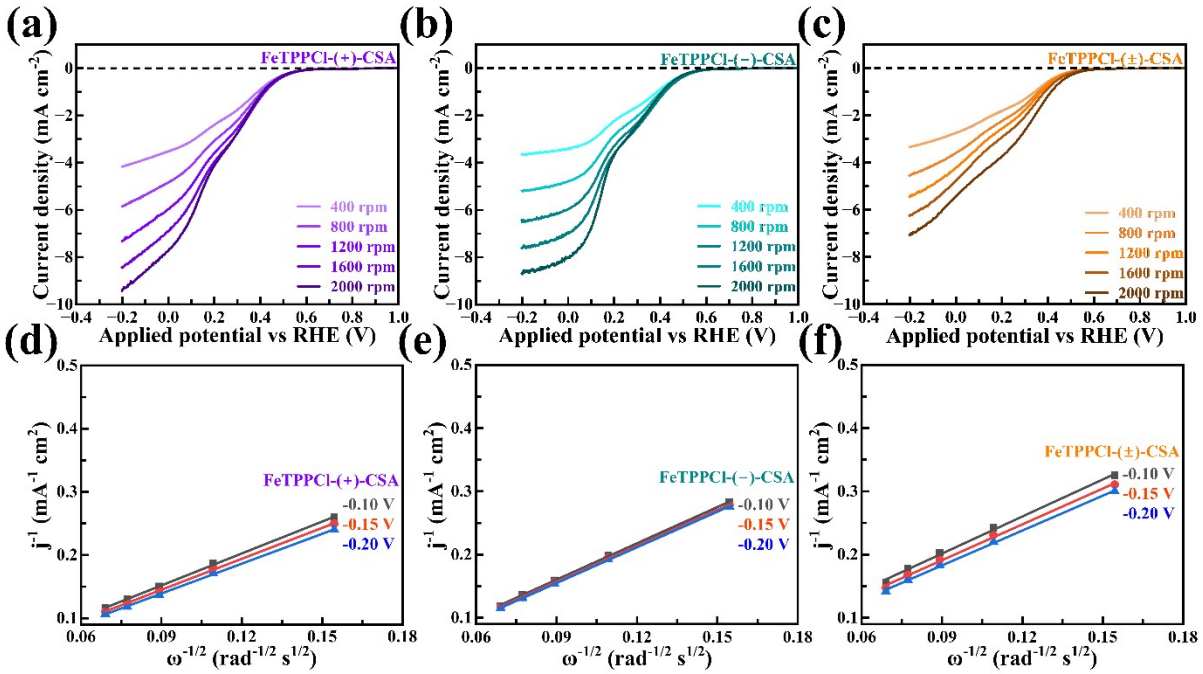

Figure S6. Cathodic polarization plots at different rpm and corresponding KL plots at different potentials in mass transport region for (a, d) FeTPPCl-(+)-CSA, (b, e) FeTPPCl-(-)-CSA, and (c, f) FeTPPCl-(±)-CSA under O_2-saturated 0.1 M $HClO_4$ environment

6. Error bar of KL plots

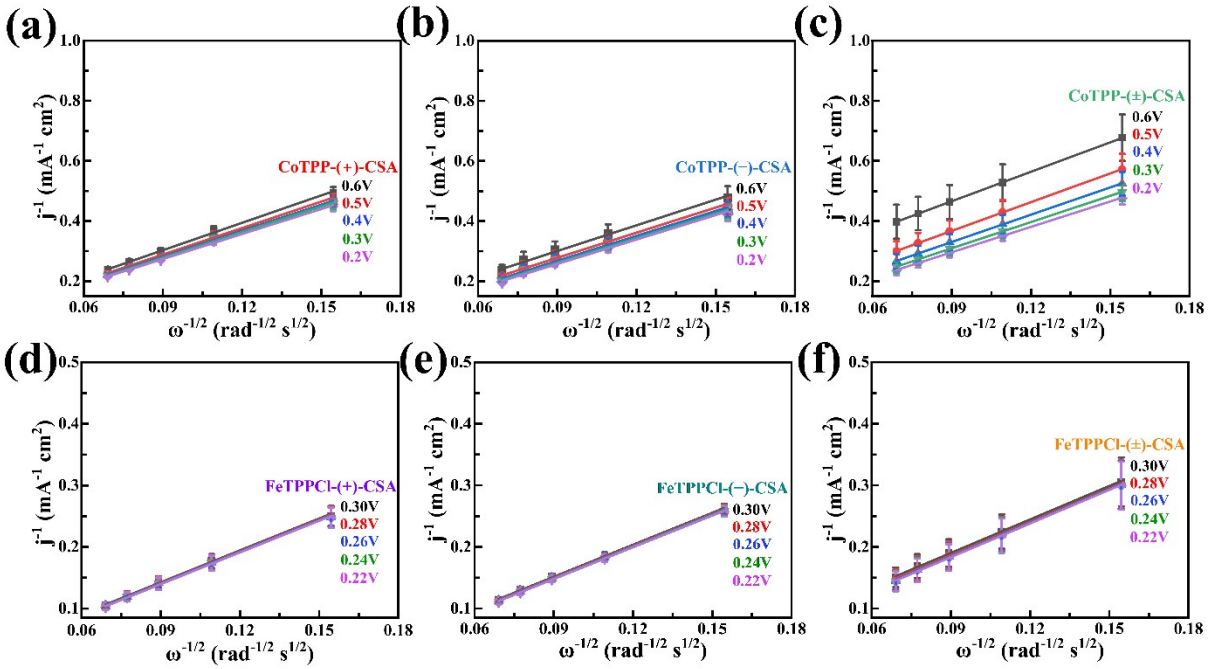

Figure S7. KL plots with error bars for chiral ((+)/(-)) and racemic (±)-CSA assembled both CoTPP and FeTPPCl moieties under alkaline (0.1 M KOH) environment.

7. Controlled experiment with metalloporphyrin (without CSA)

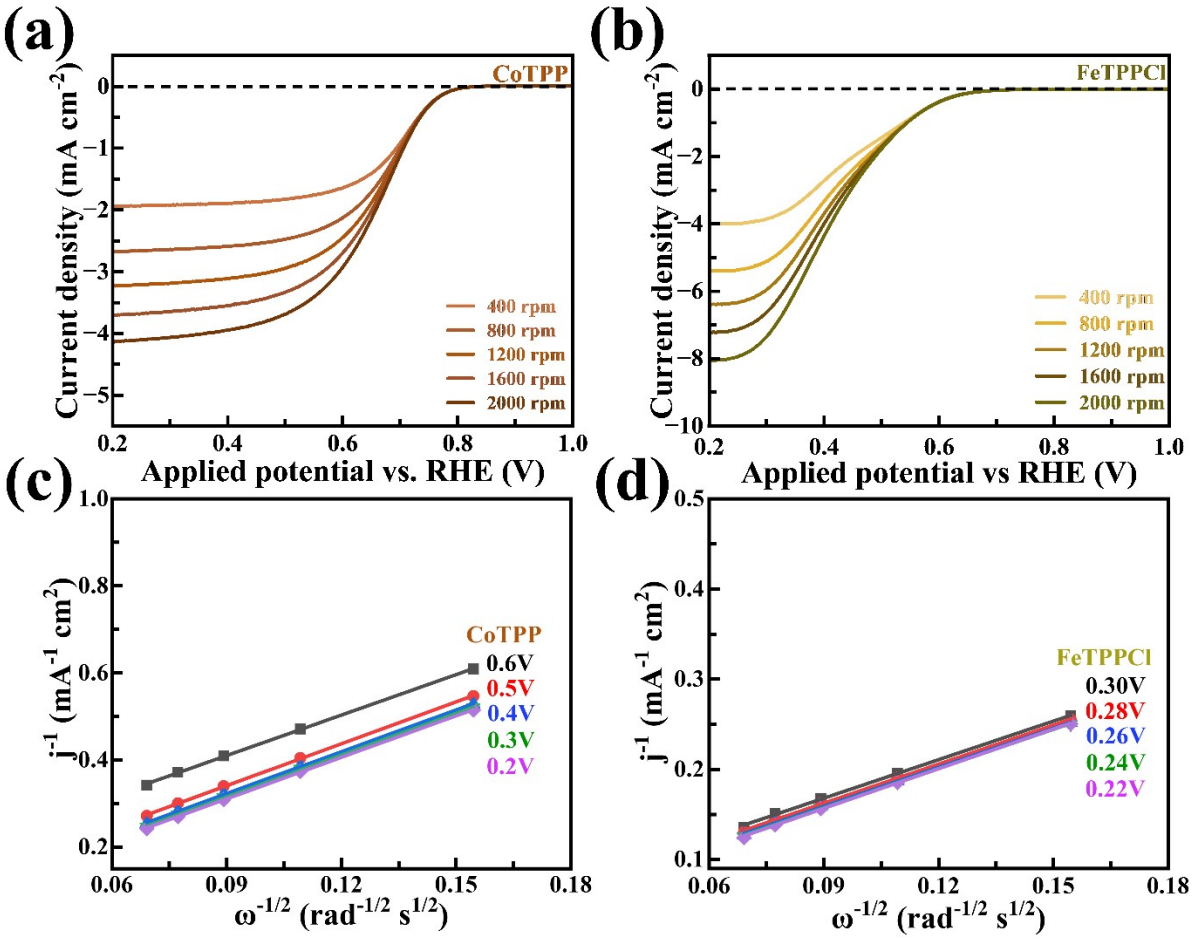

Figure S8. LSV plots at different rpm and corresponding KL plots at different potentials in the mass transport region for (a, c) CoTPP and (b, d) FeTPPCl under O_2-saturated 0.1 M KOH environment.

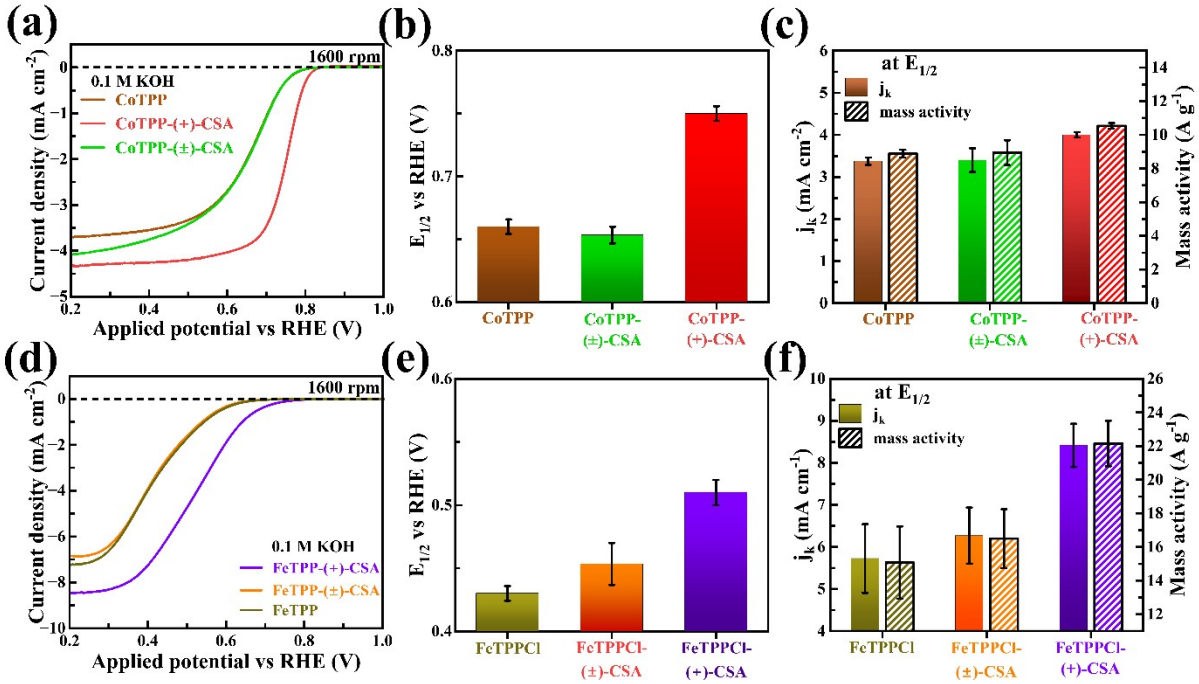

Figure S9. (a, d) Cathodic LSV plot at 1600 rpm comparing between CSA assembled and without CSA assembled metalloporphyrin moieties in O_2-saturated 0.1 M KOH electrolytes. (b, e) Half-wave potential bar plots, and (c, f) kinetic current density and mass activity bar plots at ($E_{1/2}$) for different catalysts.

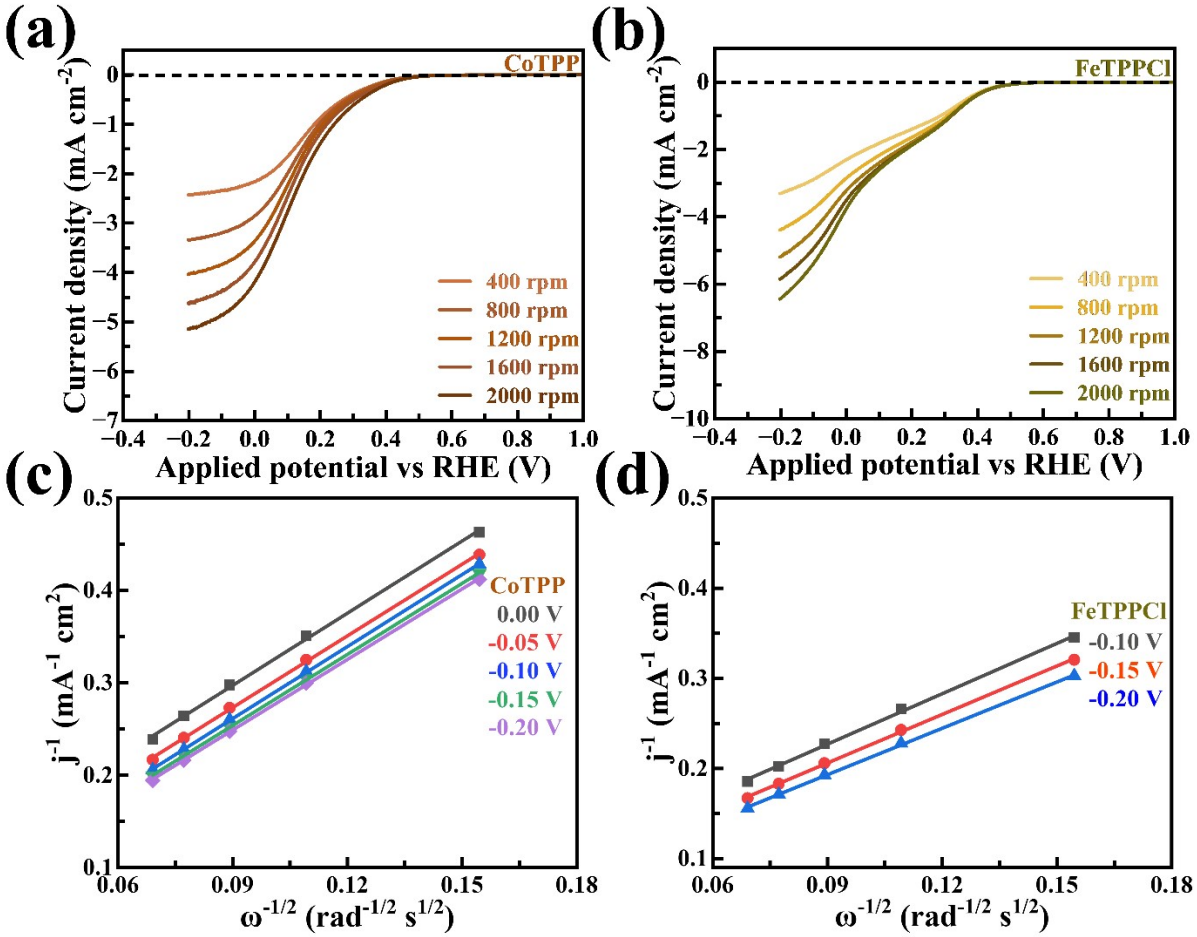

Figure S10. LSV plots at different rpm and corresponding KL plots at different potentials in the mass transport region for (a, c) CoTPP and (b, d) FeTPPCl under O_2-saturated 0.1 M $HClO_4$ environment.

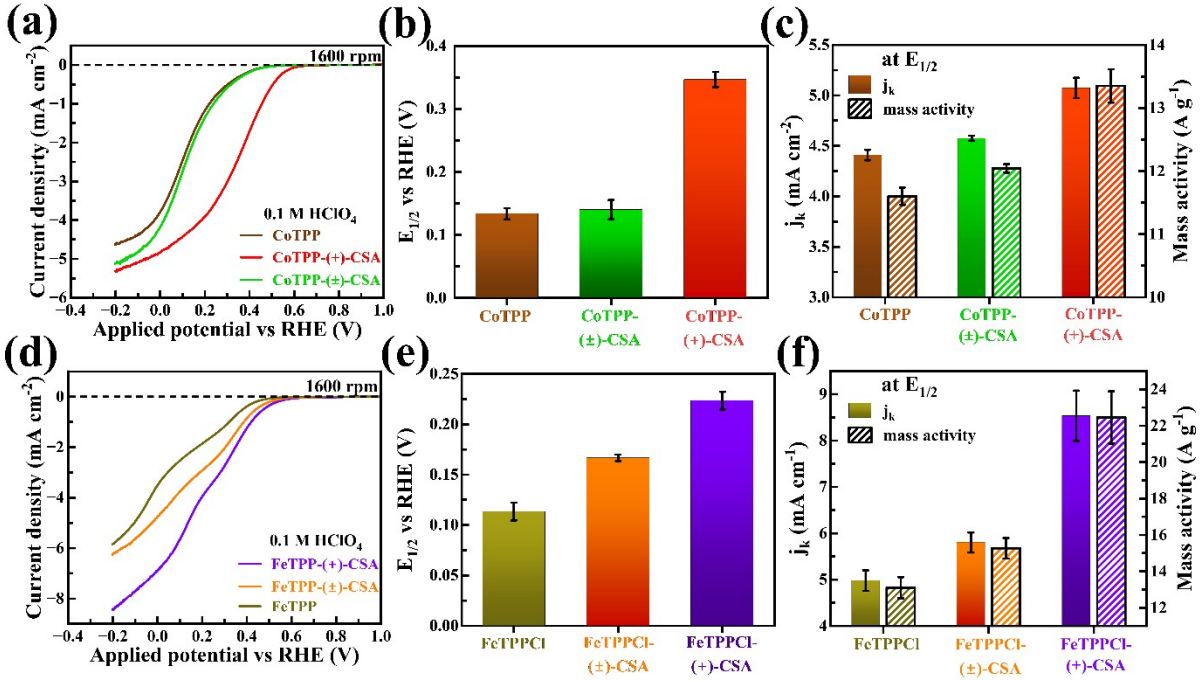

Figure S11. (a, d) cathodic LSV plot at 1600 rpm comparing between CSA assembled and without CSA assembled metalloporphyrin moieties in O_2-saturated 0.1 M $HClO_4$ electrolytes. (b, e) Half-wave potential bar plots, and (c, f) kinetic current density and mass activity bar plots at ($E_{1/2}$) for different catalysts.

8. Comparison with commercial Pt/C under alkaline medium

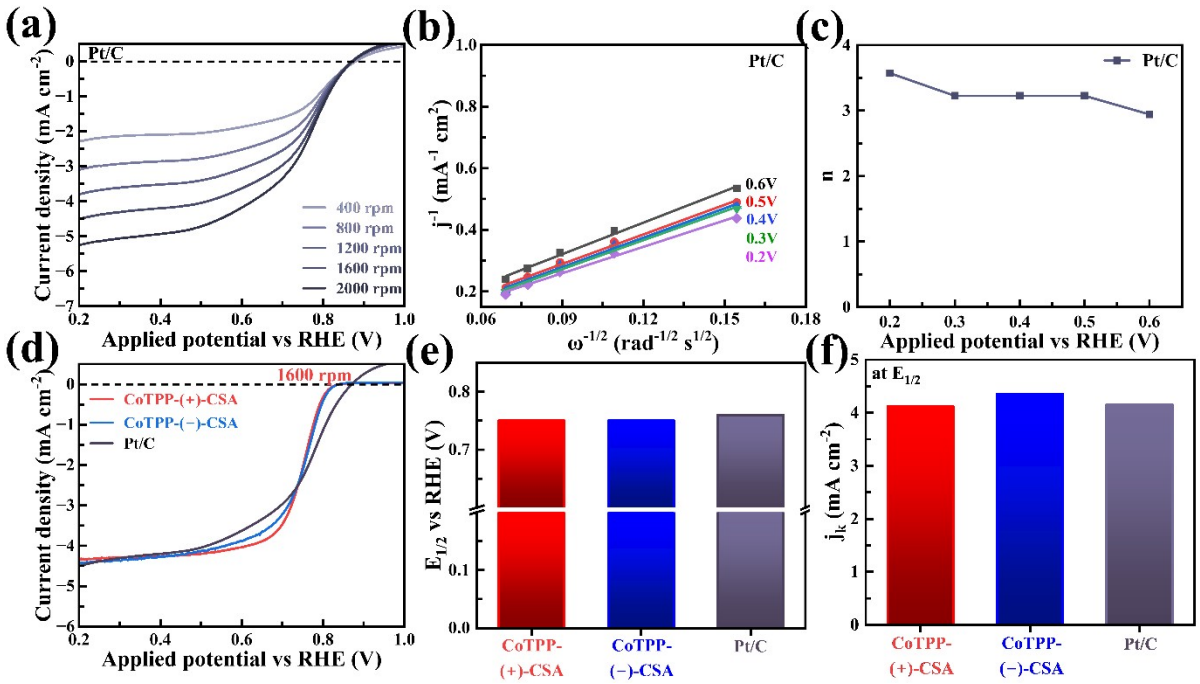

Figure S12. (a) LSV plots at different rpm, (b) corresponding KL plots in the mass transport regions, (c) electron transfer number calculated from the slope of the KL plots in the mass transport region, (d) compared LSV plots between chiral-CSA assembled CoTPP moiety and Pt/C at 1600 rpm, (e) half wave potential ($E_{1/2}$ (V) vs RHE) bar plots and (f) kinetic current density (mA cm^{-2}) bar plots at $E_{1/2}$ (V) of chiral-CSA assembled CoTPP moiety and Pt/C.

Table S1: FTIR spectra of metal-free (H_2TPP) and metalated porphyrin (CoTPP, FeTPPCl)

Wavenumber (cm^{-1})	Assigned vibration	H_2TPP	CoTPP	FeTPPCl
3309	ν_{N-H}	✓	×	×
3055	ν_{C-H}	✓	✓	✓
1593.5	$\nu_{C=C}$	✓	✓	✓
1348	$\nu_{C=N}$	✓	✓	✓
1170	$\delta_{C-H}(Ph)$	✓	✓	✓
1069	δ_{C-H} skeletal	✓	✓	✓
1001.5	ν_{Fe-N}	×	×	✓
997.1	ν_{Co-N}	×	✓	×
968.1	δ_{N-H}	✓	×	×
804	γ_{C-H}	✓	✓	✓
703.2	γ_{C-Ph}	✓	✓	✓

Note: ν: stretching mode of vibration; δ: bending mode of vibration; γ: out-of-plane mode of vibration, Ph: Phenyl group.

Table S2: Raman spectra of metalated porphyrin (CoTPP, FeTPPCl)

Wavenumber (cm^{-1})	Assigned vibration	CoTPP	FeTPPCl
362	ν_{Fe-Cl}	×	✓
392	$\nu_{Fe-N} + \nu_{Pyr\ trans}$	×	✓
1001	$\nu_{C-C} + \delta_{C-H}$	✓	✓
1077	$\rho_{H\ s} + \delta_{(C_{\beta}-H)s} + \delta_{(C-C)as}$	✓	✓
1228	ν_{C-Ph}	✓	✓
1356-1367	$\nu_{(C-N)as} + \delta_{C-H} + \nu_{(Pyr/2)s}$	✓	✓
1492	$\nu_{(C-C)s} + \delta_{C-N(H)-C}$	✓	✓
1553	$\nu_{(C-C)skeletal}$	✓	✓
3000-3100	$\nu_{aromatic\ C-H}$	✓	✓

Note: ν: stretching mode of vibration; δ: bending mode of vibration; ρ: rocking mode of vibration; s: symmetric, as: asymmetric; Ph: Phenyl group; Pyr: Pyrrole; trans: translational vibration

Table S3: Comparison of previously established metalloporphyrin ORR catalyst with chiral assembled metalloporphyrin catalyst

Catalyst	E_{onset} (V vs RHE)	Electrolytes	References
MWCNT-Co-porphyrin	0.57	1 M $HClO_4$	[4]
SWCNT/Pt	0.63	0.1 M $HClO_4$	[5]
$Ni_3(HITP)_2$	0.82	0.1 M KOH	[6]
GC/MWCNT-CoTPP	0.43 0.78	0.1 M $HClO_4$ 0.1 M KOH	[7]
GC/MWCNT-CoTHPP	0.49 0.81	0.1 M $HClO_4$ 0.1 M KOH	[7]
CoTPP-non-pyrolyzed	0.87	0.1 M NaOH	[8]
Bz-2TCoP/C aBz-TCoP/C	0.87 0.84	0.1 M KOH	[9]
EGZ1/C EGZ3/C	0.61 0.64	0.5 M H_2SO_4	[10]
cov FeTPP-CNT	0.79	0.1 M KOH	[11]
CoTPP-(+)-CSA	0.82 0.59	0.1 M KOH 0.1 M $HClO_4$	Present work
CoTPP-(-)-CSA	0.82 0.61	0.1 M KOH 0.1 M $HClO_4$	Present work
FeTPPCl-(+)-CSA	0.76	0.1 M KOH	Present work
FeTPPCl-(-)-CSA	0.75	0.1 M KOH	Present work

References:

1 A. Han, H. Jia, H. Ma, S. Ye, H. Wu, H. Lei, Y. Han, R. Cao and P. Du, *Phys. Chem. Chem. Phys.*, 2014, **16**, 11224–11232.

2 A. A. Costa, G. F. Ghesti, J. L. de Macedo, V. S. Braga, M. M. Santos, J. A. Dias and S. C. L. Dias, *J. Mol. Catal. A Chem.*, 2008, **282**, 149–157.

3 N. Bhuvanendran, S. Ravichandran, Q. Xu, T. Maiyalagan and H. Su, *Int. J. Hydrogen Energy*, 2022, **47**, 7113–7138.

4 W. Zhang, A. U. Shaikh, E. Y. Tsui and T. M. Swager, *Chem. Mater.*, 2009, **21**, 3234–3241.

5 A. Kongkanand, S. Kuwabata, G. Girishkumar and P. Kamat, *Langmuir*, 2006, **22**, 2392–2396.

6 E. M. Miner, T. Fukushima, D. Sheberla, L. Sun, Y. Surendranath and M. Dincă, *Nat. Commun.*, 2016, **7**, 10942.

7 P. K. Sonkar, K. Prakash, M. Yadav, V. Ganesan, M. Sankar, R. Gupta and D. K. Yadav, *J. Mater. Chem. A*, 2017, **5**, 6263–6276.

8 W. Orellana, C. Z. Loyola, J. F. Marco and F. Tasca, *Sci. Rep.*, 2022, **12**, 8072.

9 Y. Wei, Y. Liang, Q. Wu, Z. Xue, L. Feng, J. Zhang and L. Zhao, *Dalt. Trans.*, 2023, **52**, 14573–14582.

10 Y. Chen, L. Zhao, R. Yuan, Z. Xue, A. Wang, H. Xu, M. Cheng, H. Xu and J. Zhang, *J. Alloys Compd.*, 2022, **902**, 163790.

11 Q. Li, Y. Xu, A. Pedersen, M. Wang, M. Zhang, J. Feng, H. Luo, M.-M. Titirici and C. R. Jones, *Adv. Funct. Mater.*, 2024, **34**, 2311086.